Scalar and gravitational hair for extreme Kerr black holes

Lior M. Burko[1], Gaurav Khanna,[2,3] and Subir Sabharwal[2]

[1]*Theiss Research, La Jolla, California 92037, USA*
[2]*Department of Physics, University of Massachusetts, Dartmouth, Massachusetts 02747, USA*
[3]*Department of Physics, The University of Rhode Island, Kingston, Rhode Island 02881, USA*

For scalar perturbations of an extreme Reissner-Nordström black hole we show numerically that the Ori prefactor equals the Aretakis conserved charge. For a family of scalar or gravitational perturbations of an extreme Kerr black hole, whose members vary only in the radial location of the center of the initial packet, we demonstrate a linear relation of a generalized Ori prefactor—a certain expression obtained from the late-time expansion or the perturbation field at finite distances—and the Aretakis conserved charge. We infer that it can be established that there is an Aretakis conserved charge for scalar or gravitational perturbations of extreme Kerr black holes. This conclusion, in addition to the calculation of the Aretakis charge, can be made from measurements at a finite distance: Extreme Kerr black holes have gravitational hair that can be measured at finite distances and violates the uniqueness theorems. This gravitational hair can in principle be detected by gravitational-wave detectors.

I. INTRODUCTION AND SUMMARY

Extreme spherically symmetric and charged black holes [extreme Reissner-Nordström black holes (BHs), hereafter ERN] have been shown to carry massless scalar hair that can be measured at future null infinity ($\mathcal{I}^+$) [1]. This scalar hair is a certain quantity $s[\psi]$ which is evaluated at $\mathcal{I}^+$ and which equals the Aretakis charge, a nonvanishing quantity $H[\psi]$ which is calculated on the BH's event horizon (EH, $\mathcal{H}^+$) but vanishes if the BH is nonextreme.

Since the scalar hair at $\mathcal{I}^+$ is intimately related to the Aretakis conserved charge on $\mathcal{H}^+$, one may suspect that corresponding conserved charges for other fields on either ERN or extreme Kerr (EK) BHs may also be related to observable hair at $\mathcal{I}^+$ or be measurable at finite distances. Specifically, conserved Aretakis charges were found in ERN, in addition for massless scalar fields [2] also for massive scalar fields, for coupled linearized gravitational and electromagnetic fields [3], for charged scalar perturbations [4], and in EK for scalar [2], electromagnetic, and gravitational perturbations [5–7].

Ori showed that the Aretakis charge can also be used in order to determine a certain prefactor $e[\psi]$ in the late-time expansion of scalar field perturbation fields in ERN as measured at a finite distance [8]. (See also [9] for more detail.) Here, we first show numerically that for scalar perturbations of ERN the Ori prefactor $e[\psi]$ equals $H[\psi]$ and, therefore, can be used in order to measure the Aretakis conserved charge at a finite distance. It follows that $e[\psi]$ can be interpreted as scalar hair measured outside the BH.

We then go beyond the framework of scalar perturbations of ERN to EK and show numerically that analogous

prefactors can be formulated also for scalar and gravitational perturbations of EK. Since the value of the Aretakis charge depends on the initial data of the perturbation field, it follows that information on the preparation of the perturbation field can be inferred from the BH measurements at great distances, in apparent contradiction of the established no-hair and BH uniqueness theorems [10–12] and specifically their extensions to EK [13,14]. That is, we bring evidence that in addition to the three externally observable classical parameters, specifically the BH's mass M, charge q, and spin angular momentum a, it is in principle possible to also detect with a gravitational-wave detector the gravitational Aretakis charge of EK.

While the proposed gravitational hair of EK is intriguing as a counterexample for the uniqueness theorem, we emphasize that EK would require fine-tuning to result from a dynamical process (cf. [15]). However, for nearly extreme BHs one could identify transient gravitational hair that would persist for a duration related to its closeness to extremality, following which the hair would decay.

II. SETTING UP THE PROBLEM

Following Ori [8] we write the late-time expansion of a field $\psi^{\mathrm{I}}_{s,\ell,m}$ as

$$\psi^{\mathrm{I}}_{s,\ell,m}(t,r,\theta) = e^{\mathrm{I}}_{s,\ell,m} r(r-M)^{-p^{\mathrm{I}}_{s,\ell,m}} t^{-n^{\mathrm{I}}_{s,\ell,m}} \Theta^{\mathrm{I}}_{s,\ell,m}(\theta)$$
$$+ \mathcal{O}(t^{-n^{\mathrm{I}}_{s,\ell,m}-k^{\mathrm{I}}_{s,\ell,m}}) \quad (1)$$

in Boyer-Lindquist coordinates, where s is the field's spin, ℓ and m are the spherical harmonic numbers, and the

index I corresponds to the BH type, i.e., I = {ERN, EK}. Here, $e_{s,\ell,m}^{I}$ is a generalized Ori prefactor. The case studied in [8] corresponds to $\psi_{0,\ell,0}^{ERN}$, for which it was found that $e_{0,\ell,0}^{I} = (-4)^{\ell+1} M^{3\ell+2} e$ [8], where $e[\psi]$ is a certain pre-factor that depends on the initial data (and which is given explicitly in [8]), and $p_{0,\ell,0}^{ERN} = \ell+1$, $n_{0,\ell,0}^{ERN} = 2\ell+2$, and $\Theta_{0,0,0}^{ERN}(\theta) = 1$. The late-time expansion (1) is expected to be valid for $t \gg r_*$, where r_* is the tortoise coordinate. Specifically, we may expect r-dependent correction terms when this condition is not satisfied. Comparing [1,8] we expect that $e_{0,0,0}^{ERN}[\psi] = -4M^2 H[\psi]$.

III. NUMERICAL APPROACH

To test this prediction, and to set up the framework for generalization to EK and to gravitational perturbations, we write the $2+1$ Teukolsky equation in ERN or EK backgrounds for azimuthal ($m = 0$) modes in compactified hyperboloidal coordinates $(\tau, \rho, \theta, \varphi)$, such that $\mathcal{I}^+$ is included in the computational domain at a finite radial (in ρ) coordinate [16]. We rewrite the second-order hyperbolic partial differential equation as a coupled system of two first-order hyperbolic equations. We solve this system for the scalar field case by implementing a second-order Richtmeyer-Lax-Wendroff iterative evolution scheme [17,18]. For the gravitational case we implement a sixth-order (in ρ) weighted essentially nonoscillatory finite-difference scheme with explicit time stepping [6]. These codes converge with second-order temporally and angularly.

The initial data are compactly supported "truncated" Gaussians with nonzero initial field values on $\mathcal{H}^+$, but similar results are expected also for other forms of initial data. Specifically, in hyperboloidal coordinates (ρ, τ) (see [17] for definitions), the initially spherical ($\ell = 0$) Gaussian pulse is nonvanishing in the range $\rho/M \in [0.95, 8]$, has a width of $0.1M$ and is centered close to the BH (at $\rho/M = 1.0$, 1.1, 1.2, 1.3, 1.4 and 1.5, respectively). (The EH $\mathcal{H}^+$ is at $\rho = 0.95M$ for ERN and EK in these coordinates.) The outer boundary is located at $S = \rho(\mathcal{I}^+) = 19.0M$.

The computations were performed on IBM 32-core Power9 servers accelerated by Nvidia V100 GPGPUs. Our resolution for each production run was $\Delta\rho = M/6,400$, $\Delta\tau = M/12,800$, and $\Delta\theta = \pi/64$, which we run in quadrupole precision (128-bit, i.e., to ~30 decimal digits). The combination of quadruple-precision floating point numerics and the extremely high-resolution resulted in computationally intensive simulations, which took 2 weeks for each run to get to $t/M \sim 1600$.

IV. SCALAR PERTURBATIONS OF ERN

We calculate $e_{0,0,0}^{ERN}[\psi]$ directly from Eq. (1) and $H_{0,0,0}^{ERN}[\psi]$ from
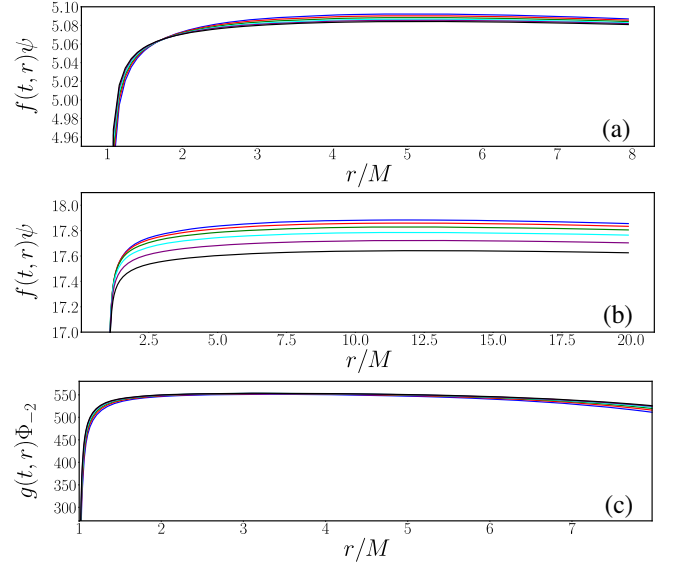
FIG. 1. The values of $e_{s,\ell,0}^{I}[\psi](t)$ as functions of r/M. These values are shown for the dataset for which at the Gaussian's center $\rho/M = 1.0$. Top panel (a): ERN with $s = 0$, $\ell = 0$. Middle panel (b): EK with $s = 0$, $\ell = 0$. Bottom panel (c): EK with $s = -2$, $\ell = 2$. The values are plotted for $t/M = 1100$ (blue line), 1200 (red line), 1300 (green line), 1400 (cyan line), 1500 (purple line), and 1600 (black line). [For panel (c) the time value was replaced with 1553.] The function $f(t, r) = (t/M)^2 (1 - M/r)$ and the function $g(t, r) = M(t/M)^6 (r/M)^4 (1 - M/r)^5$.

$$H_{0,0,0}^{I}[\psi] = -\frac{M^2}{4\pi} \int_{\mathcal{H}^+} \partial_r (r\psi) d\Omega, \qquad (2)$$

where I = ERN. To determine $e_{0,0,0}^{ERN}[\psi]$ we calculate it for a set of finite values of the time. Figure 1(a) shows $e_{0,0,0}^{ERN}[\psi]$ at a number of time values as a function of the Schwarzschild coordinate r, for the initial dataset for which the Gaussian is centered at $\rho/M = 1.0$. Notice that the numerical constancy of $(t/M)^2 (1 - M/r)\psi_{0,0,0}^{ERN}$ for small values of r/M suggests that $p_{0,0,0}^{ERN} = 1$ and $n_{0,0,0}^{ERN} = 2$, as expected from [8]. For larger values of r/M the constant value starts to vary, as expected from the expansion of [8]. Equation (1) suggests that $e_{0,0,0}^{ERN}[\psi](t)$ is time dependent and that, when $(t/M)^2 (1 - M/r)\psi_{0,0,0}^{ERN}$ is plotted as a function of inverse time, the value of k can be determined. We see in Fig. 1 that there is indeed time dependence as expected.

The time dependence of $e_{0,0,0}^{ERN}[\psi](t)$ is shown in greater detail in Fig. 2, which displays for each initial dataset the values of $e_{0,0,0}^{ERN}[\psi](t)$. We then extrapolate the values to $M/t \to 0$ by fitting to a linear function and finding the intercept and the slope to determine $e_{0,0,0}^{ERN}[\psi]$. The linearity suggests that $k_{0,0,0}^{ERN} = 1$, in agreement with [8].

The values of $e_{0,0,0}^{ERN}[\psi]$ depend on the choice of the initial dataset. In Fig. 3(a) we show $(t/M)^2 (1 - M/r)\psi_{0,0,0}^{ERN}$ for each initial dataset as functions of r/M. As the center of the
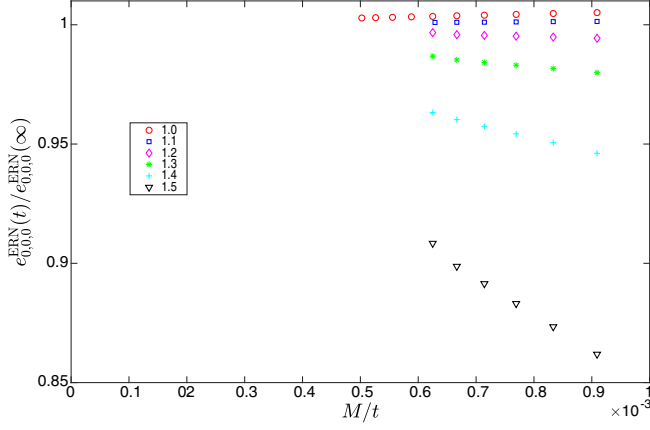
FIG. 2. The values of $e_{0,0,0}^{\mathrm{ERN}}[\psi](t)$, normalized by their values as $t \to \infty$, as functions of M/t. These values are shown for each initial dataset, parametrized by the ρ/M value at the center of the Gaussian packet.
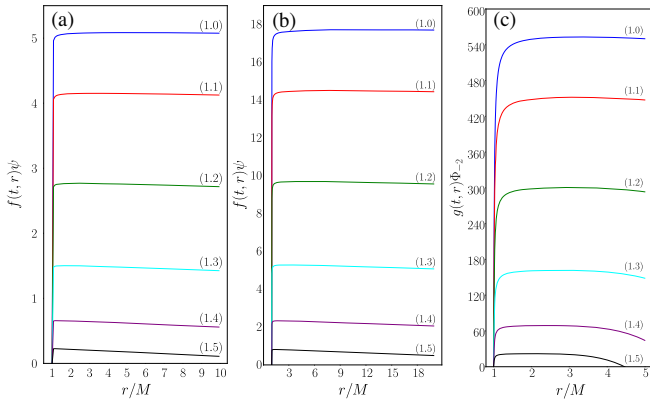
FIG. 3. The values of $e_{s,\ell,0}^{\mathrm{I}}[\psi](t/M = 1500)$ as functions of r/M, shown for each initial dataset, parametrized by the ρ/M value at the center of the Gaussian packet. Left panel (a): ERN with $s = 0, \ell = 0$. Center panel (b): EK with $s = 0, \ell = 0$. Right panel (c): EK with $s = -2, \ell = 2$.

initial Gaussian packet moves outward (to larger ρ values) the value of $(t/M)^2(1 - M/r)\psi_{0,0,0}^{\mathrm{ERN}}$ decreases.

Finally, Fig. 4(a) shows the values of $e_{0,0,0}^{\mathrm{ERN}}[\psi]$ as a function of the corresponding $H_{0,0,0}^{\mathrm{ERN}}[\psi]$ for the different datasets. Fitting our numerical data to $e_{0,0,0}^{\mathrm{ERN}}[\psi] = \alpha H_{0,0,0}^{\mathrm{ERN}}[\psi] + \beta$ we find that $\alpha = -4.0024 \pm 0.0013$ and $\beta = (1.8 \pm 9.6) \times 10^{-4}$, consistently with our expectation. The Ori prefactor e equals the Aretakis charge H.

V. SCALAR PERTURBATIONS OF EK

We next extend the analysis from the case of a scalar field in ERN to scalar and gravitational perturbations of EK. First, we set up the initial value problem for scalar field perturbations similarly as for ERN. We use the expansion (1) as an ansatz. The results for the scalar case in EK are
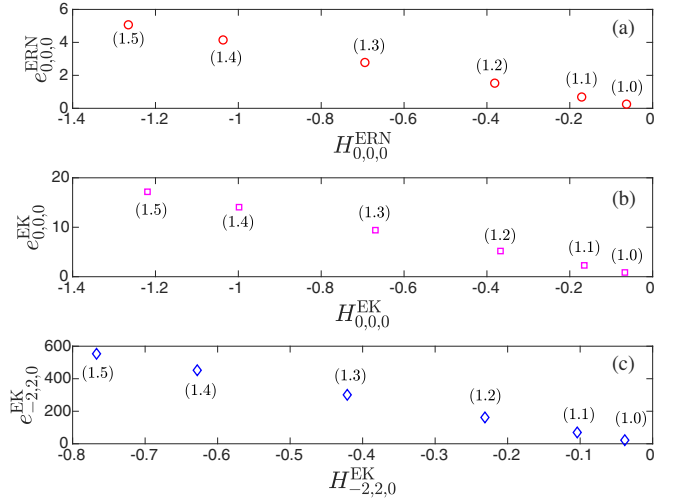
FIG. 4. The prefactor $e_{s,\ell,0}^{\mathrm{I}}[\psi]$ shown as a function of the Aretakis charge $H_{s,\ell,0}^{\mathrm{I}}[\psi]$ for the different initial datasets (parametrized with ρ/m at the center of the Gaussian initial packet). Top panel (a): ERN with $s = 0, \ell = 0$. Middle panel (b): EK with $s = 0, \ell = 0$. Bottom panel (c): EK with $s = -2, \ell = 2$.

shown in Figs. 1(b), 3(b), and 4(b). These results suggest that Eq. (1) describes well also the field for this case. Fitting the parameters to this ansatz, we find that $p_{0,0,0}^{\mathrm{EK}} = 1$ and $n_{0,0,0}^{\mathrm{EK}} = 2$. We also find that $\Theta_{0,0,0}^{\mathrm{EK}}(\theta) = 1$. To find $H_{0,0,0}^{\mathrm{EK}}[\psi]$ we again use Eq. (2) with I = EK. Seeking a linear relation of the form $e_{0,0,0}^{\mathrm{EK}}[\psi] = \alpha H_{0,0,0}^{\mathrm{EK}}[\psi] + \beta$ we find that $\alpha = -14.13 \pm 0.03$ and $\beta = -0.048 \pm 0.023$. The linear relation of $e_{0,0,0}^{\mathrm{EK}}[\psi]$ and $H_{0,0,0}^{\mathrm{EK}}[\psi]$ suggests that also in this case the Aretakis conserved charge can be measured at a finite distance and that a generalized Ori prefactor can be used in order to measure it.

VI. GRAVITATIONAL PERTURBATIONS OF EK

Finally, we consider EK gravitational perturbations with $s = -2$ and $\ell = 2$. We write the Teukolsky equation for a Kerr BH with parameters M, a for the variable Φ_{-2}, which is related to the Teukolsky function Ψ_{-2}^{K} in the Kinnersley tetrad and Boyer-Lindquist coordinates via $\Phi_{-2} = (r/\Delta^2)\Psi_{-2}^{\mathrm{K}}$, where $\Delta = r^2 - 2Mr + a^2$. Since the Weyl scalar ψ_4^{HH} in the Hartle-Hawking tetrad is related to its Kinnersley tetrad counterpart ψ_4^{K} via a type-III transformation, or $\psi_4^{\mathrm{HH}} = 4(r^2 + a^2)^2\Delta^{-2}\psi_4^{\mathrm{K}}$ [19] and since $\Psi_{-2}^{\mathrm{K}} = (r - ia\cos\theta)^4\psi_4^{\mathrm{K}}$ [20] we find that

$$\Phi_{-2} = \frac{r(r - ia\cos\theta)^4}{4(r^2 + a^2)^2}\psi_4^{\mathrm{HH}} \tag{3}$$

and use Φ_{-2} with $\ell = 2$, $m = 0$ and $a = M$ for $\psi_{-2,2,0}^{\mathrm{EK}}$. Note that at great distances, as $r \gg M$, $\psi_{-2,2,0}^{\mathrm{EK}} \sim (r/4)\psi_4^{\mathrm{HH}} \sim r\psi_4^{\mathrm{K}}$. Therefore, determination of $\psi_{-2,2,0}^{\mathrm{EK}}$ at great distances allows us to measure directly the Weyl
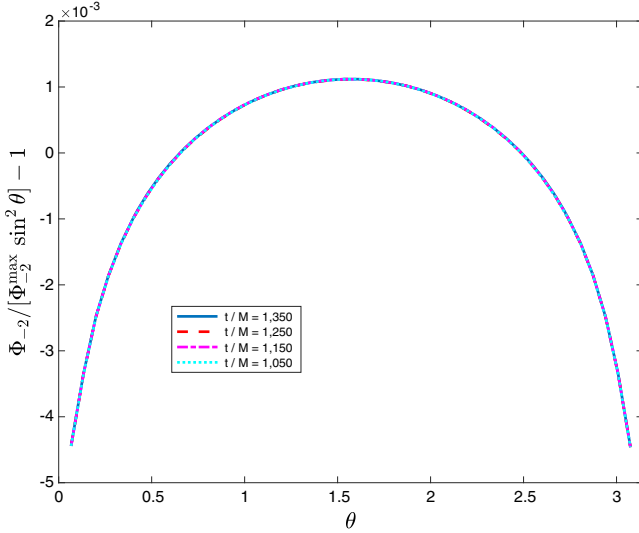
FIG. 5. The relative difference of the Weyl scalar ψ_4 (normalized by its maximal value) and $\Theta(\theta) = \sin^2 \theta$ as a function on the polar angle θ at a fixed value of $\rho/M = 2$ for four different time values, $t/M = 1050$ (dotted line), 1150 (dash-dotted line), 1250 (dashed line), and 1350 (solid line). On the scale shown these plots cannot be resolved.

scalar ψ_4^{K} in the Kinnersley tetrad. Conversely, measurement with a gravitational-wave detector at a great distance of ψ_4^{K} allows us to calculate $\psi_{-2,2,0}^{EK}$ if the distance to the source is known.

We plot Φ_{-2} for a fixed ρ as a function of θ for a set of τ values in Fig. 5. Since our angular resolution is $\Delta\theta = \pi/64$ and our code converges angularly with second order, we would expect our angular numerical error to be (a few) $\times 10^{-3}$. We find that the angular function $\Theta(\theta)$ deviates from $\sin^2 \theta$ by no more than (a few) $\times 10^{-3}$. Therefore, we could not distinguish numerically between our numerical function $\Theta(\theta)$ and $\sin^2 \theta$.

We calculate $e_{-2,2,0}^{EK}[\psi]$ directly from Eq. (1), and motivated by [3], we calculate $H_{-2,2,0}^{EK}[\psi]$ by

$$H_{-2,2,0}^{EK}[\psi] = -\frac{8}{3\pi}M^2 \int_{\mathcal{H}^+} \partial_r \Phi_{-2} d\Omega. \qquad (4)$$

(Note that ψ_4 decays to 0 at late times on $\mathcal{H}^+$.) We only calculate here the real part of ψ_4: Because of the linearity of the Teukolsky equation we can always perform a Wick rotation and obtain commensurate results for the imaginary part.

The results for the Weyl scalar ψ_4 are shown in Figs. 1(c), 3(c), and 4(c). Again, we find that the ansatz (1) describes the field behavior well. Fitting the parameters to this ansatz, we find that $p_{-2,2,0}^{EK} = 5$ and $n_{-2,2,0}^{EK} = 6$. Seeking a linear relation of the form $e_{-2,2,0}^{EK}[\psi] = \alpha H_{-2,2,0}^{EK}[\psi] + \beta$ we find that $\alpha = -729.7 \pm 0.6$ and $\beta = -6.3 \pm 0.3$. The linear relation of $e_{-2,2,0}^{EK}[\psi]$ and $H_{-2,2,0}^{EK}[\psi]$ suggest that also in this

TABLE I. The parameters used in the expansion (1), and the fitted parameters α, β in the linear relation $e_{s,\ell,0}^{I}[\psi] = \alpha H_{s,\ell,0}^{I}[\psi] + \beta$.

I	s	ℓ	p	n	$\Theta(\theta)$	α	β
ERN	0	0	1	2	1	-4.0024 ± 0.0013	$(1.8 \pm 9.6) \times 10^{-4}$
EK	0	0	1	2	1	-14.13 ± 0.03	-0.048 ± 0.023
EK	-2	2	5	6	$\sin^2 \theta$	-729.7 ± 0.6	-6.3 ± 0.3

case the Aretakis conserved charge can be measured at a finite distance and that a generalized Ori prefactor can be used in order to measure it. We summarize our results in Table I.

VII. DISCUSSION

The values for the Ori prefactor, and therefore also for the Aretakis charge—when compared between members of the same initial data family which differ from each other just by the distance of the center of the initial packet—are suggested by our results to be universal; i.e., they depend only weakly on the spin of the field and on whether the BH is ERN or EK (Fig. 3).

The linear relation of the Ori prefactor and the Aretakis conserved charge for either scalar or gravitational perturbations of EK suggests that we could make measurements at a finite distance, conclude that the BH has a conserved charge, and therefore establish also that it is an extreme BH. Moreover, by using the (numerically determined) value of the parameter α (or, in the case of scalar perturbations of ERN, its analytical value) we can calculate the value of the Aretakis charge. If the measured quantity appears to behave as for an ERN or EK for some time, and then decays as for a nonextreme BH (i.e., it is a transient behavior), we can establish that it is a nearly extreme BH [see also [21], where relevant timescales are $\sim$(a few) $\times 10^2 M$]. Since the value of the Aretakis charge depends on the perturbation field (cf. Fig. 3), and this value can be found from observations at a finite distance, this is a procedure for detecting gravitational hair of EK.

Extreme Kerr BHs that are perturbed gravitationally have hair, and this determination and also the calculation of the strength of the hair can be made at finite distances by measuring the Weyl scalar ψ_4 directly from the gravitational-wave strain. Specifically, gravitational-wave detectors can be used to measure this gravitational-field hair of extreme black holes.

This apparent contradiction of the uniqueness theorems pertains to extreme BHs, which require fine-tuning of the astrophysical processes that created them. The uniqueness theorems assume stationarity, which is violated on $\mathcal{H}^+$ because of the growth of certain transverse derivatives associated with the Aretakis phenomenon. We comment that the Aretakis phenomenon occurs only in perturbed extreme BHs, and those are characterized by decaying

external fields, consistently with the uniqueness theorems, qualitatively similar to subextremal BHs. Despite the decay of external perturbations, the conserved Aretakis charge can be measured at a great distance, thus manifesting the time dependence of transverse derivatives along $\mathcal{H}^+$. Realistic BHs are more likely to be nearly extreme and therefore would present transient hair that could in principle be detected by gravitational-wave detectors.

Work on higher-ℓ modes and nonazimuthal ($m \neq 0$) modes is currently underway. Measurement of gravitational hair of EK at $\mathcal{I}^+$ awaits further work.

ACKNOWLEDGMENTS

[1] Y. Angelopoulos, S. Aretakis, and D. Gajic, Phys. Rev. Lett. **121**, 131102 (2018).

[2] S. Aretakis, Adv. Theor. Math. Phys. **19**, 507 (2015).

[3] J. Lucietti, K. Murata, H. S. Reall, and N. Tanahashi, J. High Energy Phys. 03 (2013) 35.

[4] P. Zimmerman, Phys. Rev. D **95**, 124032 (2017).

[5] J. Lucietti and H. S. Reall, Phys. Rev. D **86**, 104030 (2012).

[6] L. M. Burko and G. Khanna, Phys. Rev. D **97**, 061502(R) (2018).

[7] S. E. Gralla and P. Zimmerman, Classical Quantum Gravity **35**, 095002 (2018).

[8] A. Ori, arXiv:1305.1564.

[9] O. Sela, Phys. Rev. D **93**, 024054 (2016).

[10] J. D. Bekenstein, Phys. Rev. Lett. **28**, 452 (1972).

[11] J. D. Bekenstein, Phys. Rev. D **5**, 1239 (1972).

[12] J. D. Bekenstein, Phys. Rev. D **5**, 2403 (1972).

[13] A. J. Amsel, G. T. Horowitz, D. Marolf, and M. M. Roberts, Phys. Rev. D **81**, 024033 (2010).

[14] P. Figueras and J. Lucietti, Classical Quantum Gravity **27**, 095001 (2010).

[15] K. Murata, H. S. Reall, and N. Tanahashi, Classical Quantum Gravity **30**, 235007 (2013).

[16] A. Zenginoğlu, Classical Quantum Gravity **25**, 145002 (2008).

[17] A. Zenginoğlu and G. Khanna, Phys. Rev. X **1**, 021017 (2011).

[18] L. M. Burko, G. Khanna, and A. Zenginoğlu, Phys. Rev. D **93**, 041501(R) (2016); **96**, 129903(E) (2017).

[19] E. Poisson, Phys. Rev. D **70**, 084044 (2004).

[20] S. A. Teukolsky, Astrophys. J. **185**, 635 (1973).

[21] L. M. Burko, G. Khanna, and S. Sabharwal, Phys. Rev. Research **1**, 033106 (2019).